



## Conventional and dynamic actinometry of discharges of hydrocarbon–oxygen–argon mixtures

Steven F. Durrant and Mário A. Bica de Moraes

Citation: *Journal of Vacuum Science & Technology A* **13**, 2513 (1995); doi: 10.1116/1.579496

View online: <http://dx.doi.org/10.1116/1.579496>

View Table of Contents: <http://scitation.aip.org/content/avs/journal/jvsta/13/5?ver=pdfcov>

Published by the AVS: Science & Technology of Materials, Interfaces, and Processing

### Articles you may be interested in

[Numerical Analysis of RF Magnetron Discharges of Oxygen/Argon Mixture](#)

AIP Conf. Proc. **663**, 865 (2003); 10.1063/1.1581632

[Conventional and dynamic actinometry of glow discharges fed mixtures of tetramethylsilane, sulfur hexafluoride, and helium](#)

J. Vac. Sci. Technol. A **16**, 509 (1998); 10.1116/1.581088

[An efficient approach to estimating thermodynamic properties of fluid mixtures in molecular simulation](#)


J. Chem. Phys. **104**, 3709 (1996); 10.1063/1.471025





[Combined molecular dynamics and energy minimization with DMSO/water mixtures as solvent. Conformation of the ArgLeuGly tripeptide](#)

AIP Conf. Proc. **330**, 409 (1995); 10.1063/1.47795

[Ionization coefficients in selected gas mixtures of interest to particle detectors](#)

J. Appl. Phys. **71**, 15 (1992); 10.1063/1.350730


Instruments for Advanced Science

<p>Contact Hiden Analytical for further details:  <b>W</b> <a href="http://www.HidenAnalytical.com">www.HidenAnalytical.com</a>  <b>E</b> <a href="mailto:info@hiden.co.uk">info@hiden.co.uk</a></p> <p><b>CLICK TO VIEW</b> our product catalogue</p>	 <p><b>Gas Analysis</b></p> <ul style="list-style-type: none"> <li>› dynamic measurement of reaction gas streams</li> <li>› catalysis and thermal analysis</li> <li>› molecular beam studies</li> <li>› dissolved species probes</li> <li>› fermentation, environmental and ecological studies</li> </ul>	 <p><b>Surface Science</b></p> <ul style="list-style-type: none"> <li>› UHV TPD</li> <li>› SIMS</li> <li>› end point detection in ion beam etch</li> <li>› elemental imaging - surface mapping</li> </ul>	 <p><b>Plasma Diagnostics</b></p> <ul style="list-style-type: none"> <li>› plasma source characterization</li> <li>› etch and deposition process reaction</li> <li>› kinetic studies</li> <li>› analysis of neutral and radical species</li> </ul>	 <p><b>Vacuum Analysis</b></p> <ul style="list-style-type: none"> <li>› partial pressure measurement and control of process gases</li> <li>› reactive sputter process control</li> <li>› vacuum diagnostics</li> <li>› vacuum coating process monitoring</li> </ul>
--	--	--	--	--

# Conventional and dynamic actinometry of discharges of hydrocarbon–oxygen–argon mixtures

Steven F. Durrant and Mário A. Bica de Moraes

*Laboratório de Processos de Plasma, Departamento de Física Aplicada, Instituto de Física Gleb Wataghin, Universidade Estadual de Campinas, 13083-970 Campinas, SP, Brazil*

(Received 1 March 1995; accepted 26 May 1995)

Actinometric optical emission spectroscopy was used in the investigation of discharges of mixtures of  $C_2H_2$ ,  $O_2$ , and Ar to determine relative concentrations of the species CH, OH, H, CO, and O, which all increase with increasing proportions of oxygen in the plasma feed,  $R_{ox}$ . The mean electron energy  $E$  and the mean electron density  $\rho$  were probed using Ar and He as actinometers. Additional measurements of the ratio of the intensities of the  $H_\alpha$  to  $H_\beta$  lines,  $I(H_\alpha)/I(H_\beta)$ , showed that  $E$  was not strongly dependent on  $R_{ox}$ . In contrast,  $\rho$  was found to fall with increasing  $R_{ox}$ . A dynamic form of actinometry was also used to determine temporal trends in the relative concentrations of the above-mentioned species following cutting of either the  $O_2$  or  $C_2H_2$  flows. On the basis of these data it is concluded that reactions involving oxygen play a major role in the production of the species CH, H, and CO. Plasma–polymer surface reactions contribute significantly to the production of the species H, CH, CO, and OH. © 1995 American Vacuum Society.

## I. INTRODUCTION

Plasma polymerization as a method for the production of thin films suited to a range of technological applications, such as protective coatings, electronic components, and permselective membranes, is well established.<sup>1,2</sup> Despite this, the processes which occur in the discharge are only partially understood. In direct current or radio frequency (rf) glow discharges, energetic electrons interact with the feed gas molecules, forming reactive species such as free radicals, ions, and excited neutrals. As a consequence of the recombination of these species, a film is formed on the inner walls of the reactor although powders or oils may also be formed,<sup>3</sup> depending on the exact deposition conditions, such as the gas feed flow rates, the applied power, and the substrate temperature.

Diverse monomers, which may be hydrocarbons,<sup>4–7</sup> or may contain oxygen,<sup>8</sup> nitrogen,<sup>9,10</sup> or silicon,<sup>11–14</sup> have been polymerized in glow discharges. Studies of the plasma polymerization of organic–inorganic mixtures, notably hydrocarbons mixed with  $N_2$ ,<sup>15</sup>  $CO$ ,<sup>16</sup> or  $O_2$ ,<sup>8,17</sup> have been reported by various investigators. This group has investigated discharge and film structures in the plasma polymerization of the mixtures  $C_2H_2$ – $SF_6$ ,<sup>18</sup>  $C_6H_6$ – $SF_6$ ,<sup>19</sup> and  $C_2H_2$ – $He$ – $N_2$ .<sup>20</sup> In such mixtures, radicals from the inorganic comonomer are usually present in the plasma and the elements of the comonomer are incorporated into the deposited film. Typically, control of the proportion of the comonomer allows some selection of the composition of the final material. For example, the degree of fluorination of films deposited from  $C_2H_2$ – $SF_6$  mixtures increases with the proportion of  $SF_6$ ,  $R_F$ , fed to the chamber.<sup>18</sup> Physical properties of the film typically depend on its elemental composition and structure, over which, as we have seen, some control is possible. Thus, for example, the refractive index of fluorinated films may be controlled by a suitable choice of  $R_F$ .<sup>18</sup>

In this work, a study of the composition of plasmas of  $C_2H_2$ – $O_2$ –Ar mixtures was made using actinometric optical

emission spectrometry to elucidate plasma processes. The introduction of a small amount of an inert gas, or actinometer, typically argon or helium, and the measurement of characteristic emissions from the actinometer and from species present in the plasma allow the determination of relative concentrations of the latter as a function of a system parameter,<sup>21,22</sup> in this work the proportion of oxygen in the feed,  $R_{ox}$ . An additional type of actinometry was also employed for the investigation of transient concentrations of species of interest in the plasma as a function of time following the interruption of one of the gas flows. As was shown recently for discharges of  $C_2H_2$ – $He$ – $N_2$  mixtures,<sup>23</sup> such *dynamic* actinometric studies may also shed light on gas-phase and surface reaction processes.

## II. EXPERIMENT

The deposition system has been described in detail elsewhere,<sup>20</sup> as has the optical equipment;<sup>18</sup> therefore a summary only follows. The discharge was maintained in a cylindrical steel chamber fitted with horizontal, water-cooled, parallel-plate electrodes connected to a rf (40 MHz) generator via a matching circuit and throughline watt meter. An rf power of 70 W was used in all experiments. Since the applied power, measured as the difference of transmitted and reflected powers, was maintained by use of the matching box, typical measurement errors are estimated to be about 5%.

Gases, of minimum purity 99.5%, were fed to the inlet at the top of the chamber from cylinders via precision mass flow controllers. The chamber was pumped continuously, via the outlet at the base of the cylinder, by a two-stage rotary pump.

A circular quartz window in the chamber wall allowed light to escape from the discharge and pass to the entrance slit of a monochromator spectrometer (focal length 1 m). Detection was by a photomultiplier tube, and the resulting

signal was passed to an electrometer and hence to a chart recorder or personal computer for display.

The following species were detected and their relative concentrations determined: CH (431.4 nm), OH (473.0 nm), H (486.1 nm), CO (519.8 nm), and O (533.1 nm). One of the conditions for the successful use of actinometry is that the threshold energies for the electronic transitions to the excited states responsible for the emissions are the same, or in practice roughly equal. For practical measurements, however, the choice of actinometer is limited to a few gases. Helium may be used but has a threshold energy of 23.73 eV (at 447.1 nm), which is far greater than the threshold energies of most of the species of interest. Argon is typically a better option: its threshold energy is 14.5 eV (at 430.0 nm). Nitrogen is sometimes used as an actinometer, but this gas cannot be considered inert because it is also incorporated into the growing polymer. For these reasons, Ar was used as an actinometer, the peak height of the emission at 430.0 nm being used to normalize the peak heights of the selected emissions of the species of interest. Helium was also introduced into the discharge and its emission at 447.1 nm measured.

### III. RESULTS AND DISCUSSION

#### A. Conventional actinometry

For this series of experiments the Ar and He flow rates were 1.9 and 0.1 sccm, respectively, while those of C<sub>2</sub>H<sub>2</sub> and O<sub>2</sub> were varied in inverse proportions in order to maintain the total flow rate constant at 8.0 sccm.

As a useful piece of background information, it is calculated that, based on the total flow rate of 8.0 sccm, the residence time in the plasma is about 2 s.

Please note that for the graphs of this section smooth curves were drawn through the data points. Thus data points not exactly on the line need not constitute poor data. Typical precisions of the peak heights were  $\pm 3\%$  the standard error of the mean ( $n=3$ ). This would be the typical error in the points of the graphs showing intensities (e.g., those of Fig. 1). The remaining graphs of this section are derived by a division of two intensities so that their typical errors are about  $\pm 4\%$ . As noted above, the gas flow rates were measured by precision mass flow controllers so that systematic errors in the flow parameters, such as the percent of oxygen in the feed, are taken to be negligible.

Figure 1 shows the relative intensity of Ar and He as a function of  $R_{ox}$ . Earlier,<sup>19</sup> the authors introduced a quantity called the *plasma activity*  $A$ , where

$$A = \rho E, \quad (1)$$

provided  $\rho$  is the mean electron density and  $E$  the mean electron energy. Thus, if  $A$  increases, either  $\rho$  or  $E$  increases (or both increase). Thus the curves show that  $A$  falls with increasing  $R_{ox}$ : either  $\rho$  or  $E$  falls (or both fall) with increasing  $R_{ox}$ . As the threshold energies for the transitions to the excited states responsible for the emissions of Ar and He measured here differ widely in energy, the similar dependence of the intensity curves on  $R_{ox}$  is indicative of a similar effect of the introduction of oxygen on electrons of diverse energy.

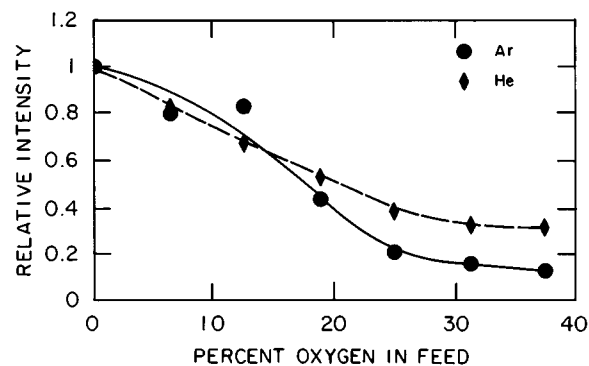


Fig. 1. Relative intensities of the actinometers Ar and He as a function of  $R_{ox}$ . Total flow rate=8 sccm; Ar flow rate=1.9 sccm; He flow rate=0.1 sccm.

An independent indication of the variation in plasma temperature with  $R_{ox}$  is obtained by monitoring two lines of a single species.<sup>24</sup> In this study, the  $H_{\alpha}$  and  $H_{\beta}$  lines at 656.2 and 486.1 nm, respectively, were measured as a function of  $R_{ox}$ . Hydrogen arises in the discharge as a fragmentation byproduct of C<sub>2</sub>H<sub>2</sub>. Figure 2 shows the variation of the ratio  $I(H_{\alpha})/I(H_{\beta})$ , where  $I$  indicates the peak height of the emission profile. Little variation is observed in the ratio as a function of  $R_{ox}$ . As the plasma activity has been shown to fall with increasing  $R_{ox}$ , it follows that higher proportions of oxygen in the feed lead to relatively low average densities of free electrons, which may be related to the electronegativity of oxygen.

Figure 3 shows the relative concentrations of CH, OH, and H as a function of  $R_{ox}$ . In what follows we designate relative concentrations by square brackets. The [CH] falls slightly and then increases rapidly as  $R_{ox}$  is increased. Since both the C<sub>2</sub>H<sub>2</sub> flow rate and the plasma activity decrease with increasing  $R_{ox}$ , the rise in [CH] at high  $R_{ox}$  must be due to increased production of CH via reactions involving oxygen in the gas phase or to the release of CH from the polymer already deposited on the electrodes and chamber walls.

The [OH] rises almost steadily with  $R_{ox}$ , while [H] shows a dependency very similar to that of [CH]. We interpret the former trend as due to the steadily increasing supply of oxygen, allowing reactions with C<sub>2</sub>H<sub>2</sub>. As both the supply of H

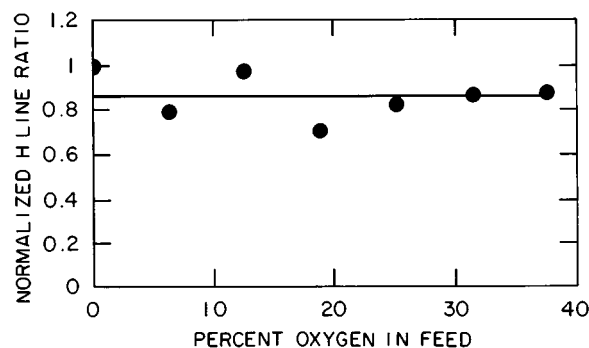


Fig. 2. Ratio of the intensities of the emissions of the  $H_{\alpha}$  and  $H_{\beta}$  lines as a function of  $R_{ox}$ . Values were normalized so that the maximum ratio equals one. Total flow rate=8 sccm; Ar flow rate=1.9 sccm; He flow rate=0.1 sccm.

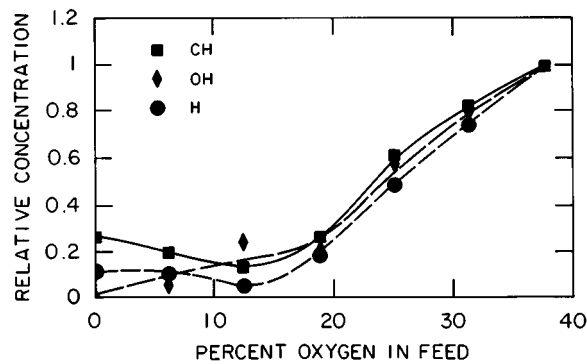


FIG. 3. Relative concentrations of the species CH, OH, and H as a function of  $R_{ox}$ . Total flow rate=8 sccm; Ar flow rate=1.9 sccm; He flow rate=0.1 sccm.

(in the form of  $C_2H_2$ ) and the plasma activity decrease with increasing  $R_{ox}$ , the rise in  $[H]$  is again probably due to reactions involving oxygen in either the gas phase or at the polymer surface or both.

Figure 4 shows the relative concentrations of CO and O as a function of  $R_{ox}$ . Both increase steadily with increasing proportions of oxygen in the feed. Since the supply of oxygen is increased, the rise in  $[O]$  is to be expected. Reactions between oxygen and carbon-containing species are very likely the mechanism responsible for the appearance of CO in the discharge. The predominant factor in the production of CO is the supply of oxygen, which outweighs the effect of the reduced plasma activity and the reduced supply of carbon in the form of monomer.

### B. Dynamic actinometry

As shown in a recent article,<sup>23</sup> actinometry may be used to determine the relative concentration of species of interest in the plasma following the cutting of one of the monomer flows. The aim here was to delineate the evolution of the relative concentrations of key plasma species with time to shed light on the influence of gas-phase and plasma-polymer surface reactions on the production of these species.

In this series of experiments the following procedure was followed. Film was deposited for 10 min under the following conditions:  $C_2H_2$  flow rate=3.0 sccm;  $O_2$  flow rate=3.0

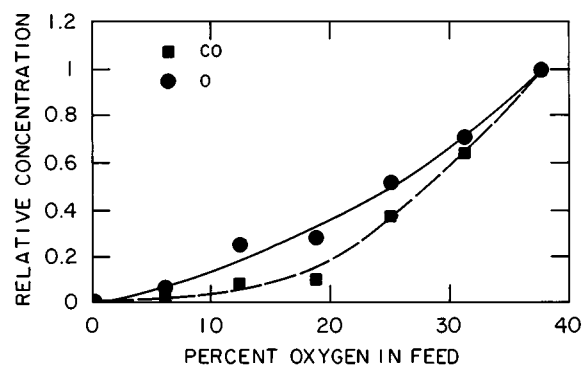


FIG. 4. Relative concentrations of the species CO and O as a function of  $R_{ox}$ . Total flow rate=8 sccm; Ar flow rate=1.9 sccm; He flow rate=0.1 sccm.

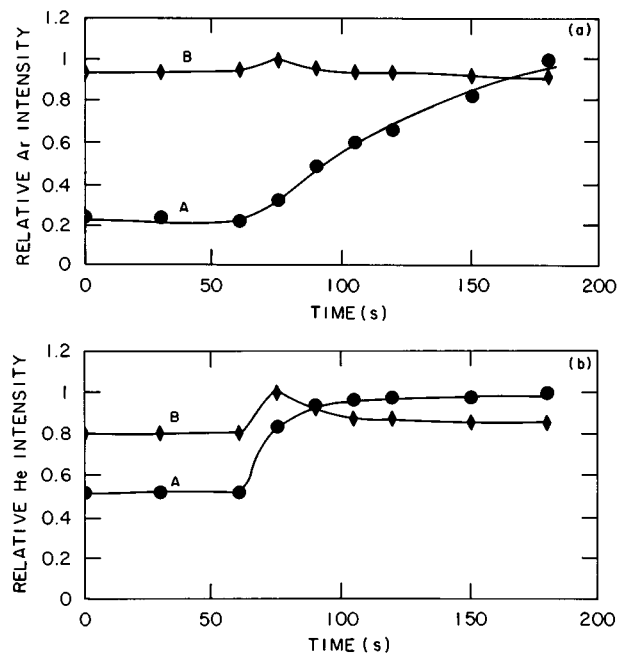


FIG. 5. Relative intensity of (a) Ar and (b) He following cutting of either (curve A) the oxygen flow or (curve B) the acetylene flow (at  $t=60$  s). Prior to deposition a film was deposited under the following conditions:  $C_2H_2$  flow rate=3.0 sccm;  $O_2$  flow rate=3.0 sccm; Ar flow rate=1.9 sccm; He flow rate=0.1 sccm; deposition time=10 min.

sccm; Ar flow rate 1.9 sccm; He flow rate=0.1 sccm. Data acquisition was begun after 9 min. After a further minute either the  $O_2$  or  $C_2H_2$  flow was cut. This procedure was repeated for measurement of the characteristic emission of each species of interest.

In the absence of the plasma the pressure in the chamber was about 48 mTorr; following ignition of the plasma, pressures of about 50 mTorr were typical. After cutting of either the  $O_2$  or the  $C_2H_2$  flow (with the plasma ignited) pressures of 22 and 42 mTorr, respectively, were observed.

Considerations similar to those given above for the conventional actinometric measurements apply to the typical precisions of the peak heights obtained by dynamic actinometry. In these experiments, however, the  $x$  variable is time. As continuous traces were made at wavelengths corresponding to the characteristic emissions, essentially an infinite number of peak heights were recorded. Therefore the error in the time coordinate of a peak height is very small but in any case smaller than the equivalent time interval occupied by the data markers (dots, diamonds, etc.) employed on the graphs.

Figures 5(a) and 5(b) show the relative intensity of Ar and He, respectively, as a function of time following the cutting of either the oxygen (curve A) or acetylene (curve B) flow.

As we can see from Fig. 5(a), when the oxygen flow rate is cut the argon intensity rises immediately and steadily, indicating an increase in the plasma activity. This is consistent with the conventional actinometry data reported in Fig. 1, where the plasma activity increases as  $R_{ox}$  decreases. Following the cutting of the acetylene flow, however, the Ar intensity is virtually constant, showing only a small rapid rise and fall, returning roughly to its original level; thus the

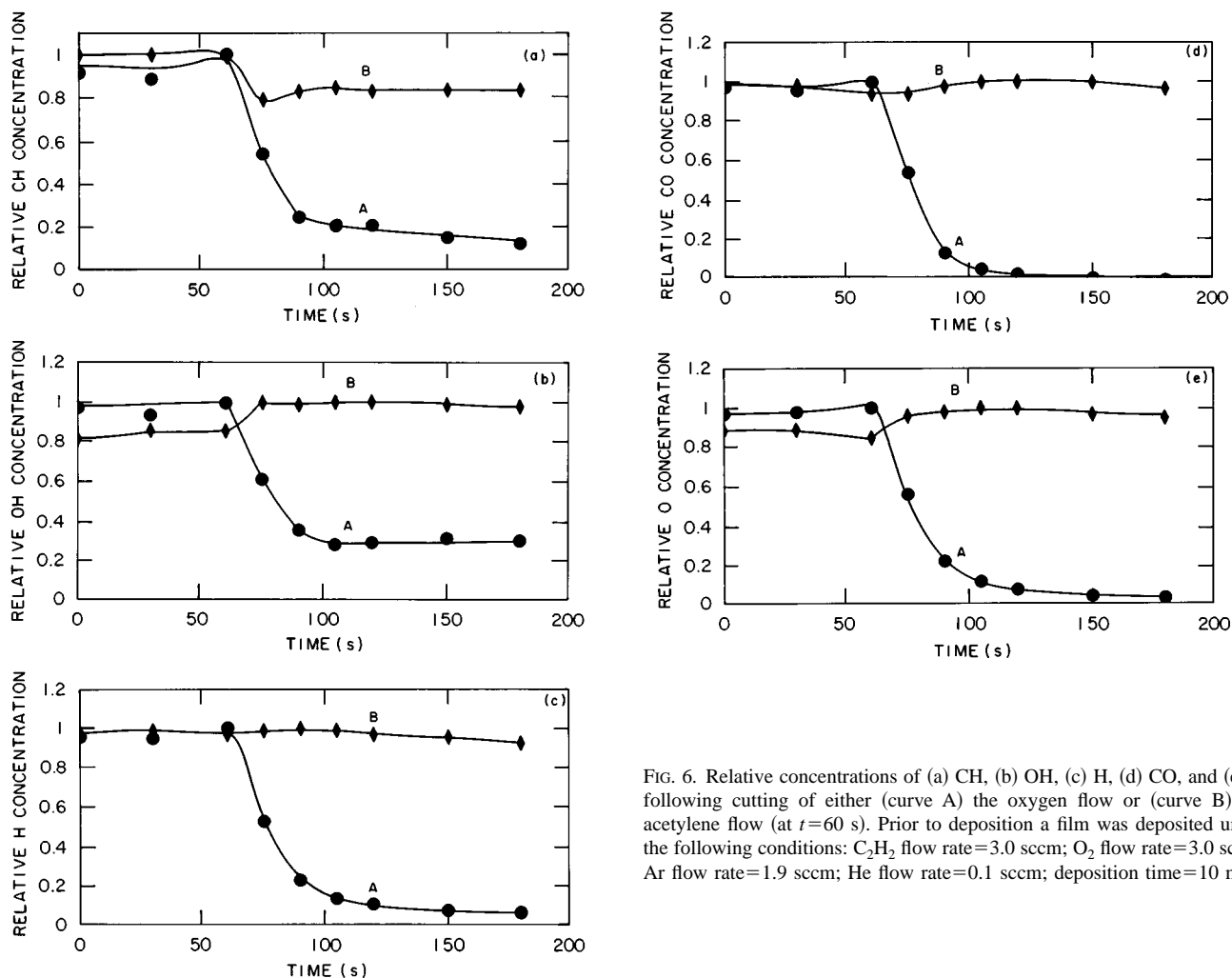


Fig. 6. Relative concentrations of (a) CH, (b) OH, (c) H, (d) CO, and (e) O following cutting of either (curve A) the oxygen flow or (curve B) the acetylene flow (at  $t=60$  s). Prior to deposition a film was deposited under the following conditions:  $C_2H_2$  flow rate=3.0 sccm;  $O_2$  flow rate=3.0 sccm; Ar flow rate=1.9 sccm; He flow rate=0.1 sccm; deposition time=10 min.

presence of  $C_2H_2$  does not greatly influence the plasma activity.

From Fig. 5(b) we see that following the cutting of the  $O_2$  flow the He intensity rises rapidly after  $t=60$  s, but is little influenced following the cutting of the  $C_2H_2$  flow. Thus although not identical, the forms of the two curves are indeed similar to those of Fig. 5(a); that is, the effect of the cutting of either the  $O_2$  or  $C_2H_2$  flow is similar for electrons in the range of the threshold energies of the actinometers, namely, 14.5–23.7 eV.

Figures 6(a)–6(e) show, respectively, the relative concentrations of the species CH, OH, H, CO, and O as a function of time following cutting of either the oxygen (curve A) or acetylene (curve B) flow.

From Fig. 6(a) (curve A) we see that the [CH] after  $t=60$  s falls extremely rapidly following the interruption of the flow of  $O_2$ . (The relative concentration obtained without  $O_2$  in the feed is very much smaller than that obtained in its presence.) This precipitous fall indicates that reactions involving oxygen are important in the rate of formation of CH. In fact, as we will show later, reactions between  $O_2$  and  $C_2H_2$  take place at a relatively high rate in the gas phase forming CO. This result strongly suggests that CH is also produced. Let us note, however, that to our knowledge there are no

metastable states of  $O_2$  with sufficient energy to produce CH directly from  $C_2H_2$ . For example, the  $^1\Delta_g$  and  $^1\Sigma^+$  metastable states of  $O_2$  have energies of 0.97 and 1.63 eV, respectively, energies far less than the  $C\equiv C$  bond energy ( $\sim 10$  eV).

In plasmas containing Ar,  $O_2$ , and  $C_2H_2$ , pathways that produce CH may include the breaking of the  $C\equiv C$  bond in  $C_2H_2$ , recombination of H and C, hydrogen extraction from  $CH_2$  species, or reactions involving  $C_2$  and H, or hydrogen-containing species. While the presence of both CH and H in the discharges was confirmed by optical emission spectroscopy, neither  $CH_2$  nor  $C_2$  was detected. However, emissions from  $CH_2$  are either weak in our discharges or suffer overlap from other emission lines. For example, the possible emission of  $CH_2$  at 537.5 nm is close to the Ar emission at 537.3 nm. Also, as oxygen is known to suppress  $C_2$  production in  $CH_4$  plasmas,<sup>24</sup> this perhaps explains the absence of confirmatory spectral evidence of the presence of  $C_2$  in our discharges.

From Fig. 6(a) (curve B) we see that when the flow of  $C_2H_2$  is cut, the [CH] falls in about 20 s to about 0.8 of its former level and is roughly stable thereafter. That [CH] does not fall to zero indicates that there are sources of CH other than gas-phase reactions starting from  $C_2H_2$ . A possible in-

terpretation of this effect is the release of CH<sub>x</sub> species from polymer deposited on the inner walls of the reactor, the energy required coming from argon metastable species. Argon has a metastable state of 11.5 eV,<sup>25</sup> an energy greater than those of the carbon bonds linking the terminations —CH<sub>3</sub> (bond energy ~4.5 eV), =CH<sub>2</sub> (bond energy ~7.5 eV), and ≡CH (bond energy ~10.0 eV) to the rest of the polymeric chains.<sup>26</sup> Energetic electrons of the plasma may also contribute to the release of CH<sub>x</sub> species from the polymer surface. Electrons are known to produce Franck–Condon transitions<sup>27</sup> in species bound to surfaces, from bonding to antibonding states, resulting in desorption.<sup>28</sup> If the carbon bond linking the CH<sub>x</sub> termination to the rest of the polymer chain suffers a transition of this kind, the CH<sub>x</sub> species may desorb from the antibonding state.

Figure 6(b) shows the temporal development of [OH] following cutting of either the O<sub>2</sub> or C<sub>2</sub>H<sub>2</sub> flow. When the O<sub>2</sub> flow is cut, [OH] falls, then stabilizes at around 25% of its original value. Thus OH must be released from the film surface. As with the species CH, this may be due to reactions with Ar metastable species or energetic plasma electrons or both.

When the flow of C<sub>2</sub>H<sub>2</sub> is cut, the concentration of OH is increased slightly, which can only be due to the greater release of OH from the polymer surface. This is not surprising because the polymer surface is bombarded with excited oxygen and argon atoms, among other species. In the case of impact by oxygen, an OH species may be directly produced; in the case of impact by argon, energy for bond breaking and the release of preformed OH species is possible. Again, energetic electrons may also release OH species.

From Fig. 6(c) we see that when the O<sub>2</sub> supply is cut, the [H] falls sharply and stabilizes at a greatly reduced concentration. The curve for [H] is strikingly similar to the corresponding curve for [CH] (following the cutting of the supply of O<sub>2</sub>). Thus the production of both CH and H depends strongly on the presence of oxygen.

The [H] does not alter greatly following the cutting of the supply of C<sub>2</sub>H<sub>2</sub>. Thus it is likely that the production of H via plasma–polymer surface reactions is of major importance.

Figure 6(d) shows the temporal variation in [CO]. The [CO] falls almost to zero in about 60 s after cutting the supply of O<sub>2</sub>. In the absence of oxygen neither gas-phase reactions via oxygen nor the production of CO via oxygen–polymer surface reactions is possible. In addition, it appears that the release of CO from the deposited material following release of the necessary energy from Ar\* species (where the asterisk indicates a metastable state), if it occurs at all, makes a negligible contribution to [CO].

In contrast to the strong influence of the presence of O<sub>2</sub> in the discharge on [CO], the absence of C<sub>2</sub>H<sub>2</sub> makes little difference to [CO]. This points to the production of CO at the polymer surface, very likely as a consequence of reactions between atomic oxygen and the carbon atoms of the polymer chains. The rate of formation of CO via gas-phase reactions is thus negligible as compared to that due to surface reactions.

As expected the [O] falls sharply when the supply of O<sub>2</sub> is cut [Fig. 6(e)]. Following the cutting of the C<sub>2</sub>H<sub>2</sub> supply, [O]

rises a little, which is probably a result of the slight increase in plasma activity obtained in the absence of C<sub>2</sub>H<sub>2</sub> [see Fig. 5(b)].

#### IV. CONCLUSIONS

In plasmas of mixtures of C<sub>2</sub>H<sub>2</sub>, O<sub>2</sub>, and Ar, increasing proportions of oxygen lead to lower plasma activities. As was shown by the measurement of the ratio of the intensities of the hydrogen lines,  $I(H_{\alpha})/I(H_{\beta})$ , the plasma temperature is not a strong function of the proportion of oxygen in the feed,  $R_{ox}$ , and the mean electron density falls with increasing  $R_{ox}$ . Despite this, conventional actinometry revealed that the relative concentrations [CH], [OH], [H], [CO], and [O] increase with increasing  $R_{ox}$ . Some increase in the concentrations of oxygen-containing species is expected as  $R_{ox}$  is increased. However, simultaneous with the increase in the supply of oxygen, the supply of C and H in the form of a monomer decreases. This factor, together with the reduced plasma activity, must tend to reduce the concentrations of the species H and CH. The concentrations of these species, though, are observed to increase, owing to reactions involving oxygen.

Using a dynamic actinometric technique, in which the flow of oxygen was interrupted, we have shown that reactions involving oxygen or oxygen-containing species are essential to the formation of the CH, H, and CO species. The existence of relatively high concentrations of the species H, CH, CO, and OH without C<sub>2</sub>H<sub>2</sub> in the plasma feed suggests that plasma–polymer surface reactions play a very important role in their release into the discharge. Energetic plasma species such as electrons and argon metastable species may supply the energy necessary to release the above-mentioned species from the film surface.

In addition to the specific clues concerning reaction mechanisms in C<sub>2</sub>H<sub>2</sub>-O<sub>2</sub>-Ar plasmas obtained here, the dynamic actinometric method promises to be a useful additional tool for plasma diagnosis.

As illustrated by Prohaska and Nickoson<sup>17</sup> for ethylene–oxygen plasmas, the inclusion of oxygen as a comonomer leads to its incorporation into the deposited material, which modifies film properties such as the dielectric constant. A study of the structural and optical properties of films deposited from C<sub>2</sub>H<sub>2</sub>-O<sub>2</sub>-Ar mixtures is also to be reported.<sup>29</sup>

#### ACKNOWLEDGMENTS

The authors thank the Fundação de Amparo à Pesquisa do Estado de São Paulo and the Conselho Nacional de Desenvolvimento Científico e Tecnológico of Brazil for financial support.

<sup>1</sup>H. Yasuda, *Plasma Polymerization* (Academic, New York, 1985).

<sup>2</sup>*Plasma Deposition, Treatment and Etching of Polymers*, edited by R. d'Agostino (Academic, New York, 1990).

<sup>3</sup>R. Liepins and K. Sakaoku, *J. Appl. Polym. Sci.* **16**, 2633 (1972).

<sup>4</sup>H. Yasuda, H. C. Marsh, M. O. Bumgarner, and N. Morosoff, *J. Appl. Polym. Sci.* **19**, 2845 (1975).

<sup>5</sup>H. Kobayashi, A. T. Bell, and M. Shen, *Macromolecules* **7**, 277 (1974).

<sup>6</sup>A. Dilks, S. Kaplan, and A. Van Laeken, *J. Polym. Sci. Polym. Chem. Ed.* **19**, 2987 (1981).

- <sup>7</sup>H. Yasuda and T. Hsu, *J. Polym. Sci. Polym. Chem. Ed.* **15**, 81 (1977).
- <sup>8</sup>S. F. Durrant, N. Marçal, P. R. Pedrosa, E. C. Rangel, and M. A. Bica de Moraes, in Proceedings of the CLACSA-8, Cancun, Mexico, September 1994 (unpublished).
- <sup>9</sup>Z. Novotny and H. Biederman, *Vacuum* **39**, 17 (1989).
- <sup>10</sup>F. Fracassi, R. d'Agostino, P. Favia, and M van Sambeck, *Plasma Sources Sci. Technol.* **2**, 106 (1993).
- <sup>11</sup>J. L. C. Fonseca, D. C. Apperley, and J. P. S. Badyal, *Chem. Mater.* **5**, 1676 (1993).
- <sup>12</sup>J.-L. Dorier, Ch. Hollenstein, A. A. Howling, and U. Kroll, *J. Vac. Sci. Technol. A* **10**, 1048 (1992).
- <sup>13</sup>K. W. Kerstenberg and W. Beyer, *J. Appl. Phys.* **62**, 1782 (1987).
- <sup>14</sup>M. Morra, E. Occhiello and F. Garbassi, *J. Appl. Polym. Sci.* **48**, 1331 (1993).
- <sup>15</sup>M. Ricci, M. Trinquecoste, F. Auguste, R. Canet, and P. Delhaes, *J. Mater. Res.* **8**, 480 (1993).
- <sup>16</sup>H. Yasuda and H. C. Marsh, *J. Appl. Polym. Sci.* **19**, 2981 (1975).
- <sup>17</sup>G. W. Prohaska and C. G. Nickoson, *J. Polym. Sci. A, Polym. Chem.* **27**, 2633 (1989).
- <sup>18</sup>S. F. Durrant, R. P. Mota, and M. A. Bica de Moraes, *J. Appl. Phys.* **71**, 448 (1992).
- <sup>19</sup>S. F. Durrant, R. P. Mota, and M. A. Bica de Moraes, *Thin Solid Films* **220**, 295 (1992).
- <sup>20</sup>S. F. Durrant, N. Marçal, S. G. Castro, R. C. G. Vinhas, M. A. Bica de Moraes, and J. H. Nicola, *Thin Solid Films* **259**, 139 (1995).
- <sup>21</sup>J. W. Coburn and M. Chen, *J. Appl. Phys.* **51**, 3134 (1980).
- <sup>22</sup>R. d'Agostino, F. Cramarossa, and F. Illuzzi, *J. Appl. Phys.* **61**, 2754 (1987).
- <sup>23</sup>S. F. Durrant, E. C. Rangel, and M. A. Bica de Moraes, *J. Vac. Sci. Technol. A* **13**, 1901 (1995).
- <sup>24</sup>W. Zhu, A. Inspektor, A. R. Badzian, T. McKenna, and R. Messier, *J. Appl. Phys.* **68**, 1489 (1990).
- <sup>25</sup>M. Hudis, in *Plasma Treatment of Solid Materials in Techniques and Applications of Plasma Chemistry*, edited by J. R. Hollahan and A. T. Bell (Wiley, New York, 1974), p. 126.
- <sup>26</sup>H. B. Gray, *Electrons and Chemical Bonding* (Benjamin, New York, 1964), p. 163; H. Yasuda, in Ref. 1, p. 74.
- <sup>27</sup>H. S. W. Massey and E. H. S. Burhop, *Electronic and Ionic Impact Phenomena* (Oxford University Press, Oxford, 1952).
- <sup>28</sup>T. E. Madey and J. T. Yates, Jr., *J. Vac. Sci. Technol.* **8**, 525 (1971).
- <sup>29</sup>S. F. Durrant, S. G. Castro, J. Cisneros, N. C. da Cruz, and M. A. Bica de Moraes, *J. Vac. Sci. Technol. A* (submitted).